

# **Electromigration-Induced Plastic Deformation in Passivated Metal Lines**

B. C. Valek *et al.*

*Submitted to Applied Physics Letters*

---

*Stanford Linear Accelerator Center, Stanford University, Stanford, CA 94309*

Work supported by Department of Energy contract DE-AC03-76SF00515.

# Electromigration-Induced Plastic Deformation in Passivated Metal Lines

B.C. Valek, J. C. Bravman

*Dept. Materials Science & Engineering, Stanford University, Stanford CA 94305*

N. Tamura, A.A.MacDowell, R. S. Celestre, H.A. Padmore,

*Advanced Light Source, 1 Cyclotron Road, Berkeley CA 94720*

R. Spolenak , W.L. Brown

*Bell Laboratories, Lucent Technologies, Murray Hill NJ 07974*

B.W. Batterman , J. R. Patel

*Advanced Light Source, 1 Cyclotron Road, Berkeley CA 94720 , and Stanford*

*Synchrotron Radiation Laboratories , P.O.BOX 4349, Stanford CA 94309*

## Abstract

We have used scanning white beam x-ray microdiffraction to study microstructural evolution during an *in-situ* electromigration experiment on a passivated Al(Cu) test line. The data show plastic deformation and grain rotations occurring under the influence of electromigration, seen as broadening, movement, and splitting of reflections diffracted from individual metal grains. We believe this deformation is due to localized shear stresses that arise due to the inhomogeneous transfer and deposition of metal along the line. Deviatoric stress measurements show changes in the components of stress within the line, including relaxation of stress when current is removed.

Electromigration (EM) is a phenomenon that occurs when extremely high current densities ( $j \sim 10^6$  A/cm<sup>2</sup>) lead to mass transport of metal within integrated-circuit metallizations.<sup>1</sup> Failure of the interconnect can be caused by open circuit voiding or short circuit extrusions of the metal. The evolution of stress caused by EM in metallic interconnects is an important topic in microelectronics reliability.<sup>2</sup> Large stresses can develop in the line because of the transport of metal in a confined space. A great deal of research has been conducted in an attempt to understand the role of stress and stress gradients during EM and several models have been proposed.<sup>3,4,5</sup> Experimental verification of these models has proven difficult due to the challenge of measuring stress in passivated interconnect structures with the necessary spatial resolution.

With recent advances in synchrotron and x-ray optics technology, x-ray microbeams have proven useful in the study of EM. X-rays are ideal for interconnect studies, as they can be focused on the order of the grain size and can penetrate any dielectric covering the line, unlike electron beams, which are only sensitive to the sample surface. Several groups have recently reported results using various x-ray microbeam techniques.<sup>6,7,8</sup> In this letter, we report results using scanning white beam x-ray microdiffraction, which allows for mapping the complete orientation and deviatoric stress/strain tensor of micron-scale grains within a passivated interconnect line. Additionally, the constituent Laue reflections for a given grain can yield information about plastic deformation that may occur during EM.

This experiment was conducted at Beamline 7.3.3 at the Advanced Light Source synchrotron in Berkeley, CA. A detailed description of the beamline is available in a recent article.<sup>9</sup> A white x-ray beam (6-14 keV) is focused to a spot size of 0.8 x 0.8  $\mu\text{m}$

using a Kirkpatrick-Baez mirror pair. The sample, mounted on a piezoelectric positioning stage, is scanned beneath this x-ray spot. Data is collected as an array of white beam (or Laue) diffraction patterns in reflection mode from individual crystallites within the sample via a CCD detector. These Laue patterns are automatically analyzed with custom software for both orientation and deviatoric stress/strain.

The sample investigated here is a sputtered Al(0.5 wt.% Cu) two level electromigration test structure. The test line has dimensions of 4.1  $\mu\text{m}$  in width, 30  $\mu\text{m}$  in length and 0.75  $\mu\text{m}$  in thickness. There are two shunt layers of Ti at the bottom and the top of the lines (thicknesses are 450  $\text{\AA}$  and 100  $\text{\AA}$  respectively). The lines are passivated with 0.7  $\mu\text{m}$  of  $\text{SiO}_2$  (PETEOS). Tungsten vias at either end of the line connect to a lower metallization level, which in turn connects to unpassivated bond pads for electrical connection to be made. The sample was annealed at 390°C for 30 minutes in a rough vacuum prior to the experiment.

The electromigration test was conducted at 205°C. Current and voltage across the sample were monitored at 10 second increments. The sample was scanned in 0.5  $\mu\text{m}$  steps, 15 steps across the width of the line and 65 steps along the length of the line, for a total of 975 CCD frames collected. A complete set of CCD frames takes about 4 to 5 hours to collect (depending on the reliability of the synchrotron source). The exposure time was 5 seconds plus about 10 seconds of electronic readout time for each frame. In this manner, information regarding the deviatoric stress/strain state, orientation, and plastic deformation for each grain in the sample was collected for each time step during the experiment. The current was ramped up to +30 mA ( $j = 0.98 \text{ MA cm}^{-2}$ ) over the

course of 24 hours (in 10 mA increments), then turned off for 12 hours, and finally reversed to -30 mA for the next 18 hours.

Fig. 1 shows the evolution of the (222) and (113) Laue reflections for several grains in the line during the *in-situ* EM experiment. Because a given Laue reflection will appear in many frames, only the reflections from the center of the grains are shown. The reflections have been converted to q-space (reciprocal space), with the x-axis along the length of the line, the y-axis across the line, and the z-axis normal to its surface. It is clear that some of the reflections are broadening as the EM test progresses, while some grains even split into clearly defined subgrains. On the CCD frame, the broadening is manifested in different directions for different planes. When converted to q-space, the broadening and splitting are seen to be in the same direction, which is across the length of the line. The deformation takes place in this manner along most of the line, although some grains at the very ends of the line have a component of deformation along the length of the line.

The degree of plastic deformation is dependent on the position of the grain within the line. The width of a Laue reflection contains information on the dislocation density within a grain. The peak broadening during electromigration can be quantified by defining  $\Delta\theta$  as the difference between the full width at half maximum (FWHM) of the peaks plotted in theta-chi space. Theta is defined as the Bragg angle, and chi is the angle within the plane perpendicular to the incident beam. The peak broadening is strongest in the theta direction, which is across the length of the line. If we plot  $\Delta\theta$  of the (222) peak for several grains along the line, we can see a clear trend in the amount of peak broadening in a grain versus position in the line. Fig. 2(a) shows that plastic deformation

increases as the anode is approached after 24 hours of electromigration (current during scan is +30 mA). The scatter in  $\Delta\theta$  is most likely caused by inhomogeneous deposition of metal within the line, resulting from flux divergences along the length of the line. After current reversal, plastic deformation continues and many grains are further divided into subgrains, as seen in Fig. 1.

In addition to peak broadening and splitting, grain rotations are also visible in Fig 1. These rotations are not due to the entire sample rotating, which would be evident via movement of the silicon background Laue pattern. In fact, many grains rotate in opposite directions from one another. Using the variation in intensity of a Laue reflection from a grain, we can estimate the size, shape, and location of the grain within the line. Fig. 2(b) is a plot of the change in position of the (222) Laue reflection for grains on either side of the line versus distance along the line. Grains in the top half of the line ( $y > 0$ , if  $y = 0$  is in the middle of the line width) rotate in the  $-\theta$  direction, while those on the bottom half ( $y < 0$ ) rotate in the  $+\theta$  direction. Transport of material towards the anode causes a convex bowing of the line that increases as the anode is approached. Others have reported this type of bowing in post-mortem examination of EM specimens.<sup>10</sup>

Fig. 3 is a plot of the average deviatoric stresses and the average maximum resolved shear stress (MRSS)<sup>11</sup> in the line versus time during the experiment. These stresses are the average of all grains in the line at each time step. The MRSS is calculated for the (111) $\langle 110 \rangle$  type slip system. In the following, X is in the direction of the line, Y is across the line, and Z is the normal to the sample surface. During the ramping of the current to +30 mA, the average of the deviatoric stress components  $\langle \sigma'_{xx} \rangle$  and  $\langle \sigma'_{yy} \rangle$  increase, while  $\langle \sigma'_{zz} \rangle$  decreases. The average MRSS in the line

increases during the experiment. Removing the current from the sample relaxes these stresses, while reversing the current restores the stresses. While we see a change in the average stress values at each time step, we do not see a gradient in the stress values along the length of the line. We do not have information on the hydrostatic stress in the line. The stresses were also measured for a control sample that was at the same temperature as the EM sample, but had no current applied. The stresses remain constant in this sample and no peak broadening or grain rotations are observed.

We believe that the evidence from this experiment clearly shows that plastic deformation is an important process occurring during EM. Metal is being removed from near the cathode and deposited towards the anode. Flux divergences along the line lead to inhomogeneous metal accumulations at various locations. It is believed that these metal accumulations change the stress state of the surrounding grains, increasing local shear stresses that are then relieved via plastic deformation. Because plastic deformation will not relieve the hydrostatic stress, a gradient in hydrostatic stress can still exist. It should be noted that post-electromigration examination of the sample revealed no hillocks or extrusions. This is significant because it shows that the deformation was occurring within a closed volume and material was not allowed to escape. Electroplasticity is the phenomenon of dislocation motion and multiplication due to an applied current. Baker *et al.* have investigated electroplasticity as it relates to electromigration in unpassivated interconnects, but did not find any significant effect.<sup>12</sup> The fact that we see a gradient in both peak broadening and grain rotation indicates that the plastic deformation is most likely due to induced local shear stresses, rather than electroplasticity.

Barabash *et al.* have recently shown that white beam x-ray microdiffraction can be useful for the analysis of dislocation structures<sup>13</sup>. The majority of peak broadening occurs across the width of the line, rather than along the length of the line. The broadening and splitting of the Laue reflections suggests a process in which geometrically necessary dislocations are produced within the grain and then coalesce into geometrically necessary boundaries formed by tilt dislocation walls. These dislocations have cores that run parallel to the applied current, and therefore may serve as new fast diffusion paths along the line.

In conclusion, we have used white beam x-ray microdiffraction to show that plastic deformation occurs during electromigration within passivated metallic interconnects. Peak broadening and grain rotations reveal gradients in the amount of plastic deformation along the line. *In-situ* stress measurements show an overall change in the average deviatoric stresses, which relax when the current is removed, but are restored by reversing the current.

#### ACKNOWLEDGEMENTS

The Advanced Light Source is supported by the Director, Office of Science, Office of Basic Energy Sciences, Materials Sciences Division, of the U.S. Department of Energy under Contract No. DE-AC03-76SF00098 at Lawrence Berkeley National Laboratory. We would like to thank Intel Corporation for generous funding and support.



## REFERENCES

1. J.F. Lloyd, J. Phys. D **32**, R109 (1999)
2. I.A. Blech, J. Appl. Phys. **47**, 1203 (1976)
3. M.A. Korhonen, P. Borgesen, K.N. Tu, and C. Li, J. Appl. Phys. **73**, 3790 (1993)
4. R.J. Gleixner and W.D. Nix, J. Appl. Phys. **83**, 3595 (1998)
5. M.P. Surh, J. Appl. Phys., **85**, 8145 (1999)
6. G. S. Cargill III, *Stress-Induced Phenomena in Metallization*, 6<sup>th</sup> International Workshop, Editors S.P. Baker, M.A. Korhonen, E. Arzt, and P.S. Ho, 193-204 (2002)
7. H.H. Solak, Y. Vladimirov, F. Cerrina, B. Lai, W. Yun, Z. Cai, P. Ilinski, D. Legnini, and W. Rodrigues, J. Appl. Phys. **86**, 884 (1999)
8. P.C. Wang, I.C. Noyan, S.K. Kildor, J.L. Jordan-Sweet, E.G. Liniger, and C.K. Hu, Appl. Phys. Lett. **78**, 2712 (2001)
9. N. Tamura, R.S. Celestre, A.A. MacDowell, H.A. Padmore, R. Spolenak, B.C. Valek, N. Meier Chang, A. Manceau, and J.R. Patel, Rev. of Scientific Instrum., **73**, 1369 (2002).
10. J.C. Doan, S. Lee, S.H. Lee, P.A. Flinn, J.C. Bravman, and T.N. Marieb, J. Appl Phys. **89**, 7797 (2001)
11. B.C. Valek, N. Tamura, R. Spolenak, A.A. MacDowell, R.S. Celestre, H.A. Padmore, J.C. Bravman, W.L. Brown, B.W. Batterman, and J.R. Patel, Mat. Res. Soc. Symp. Proc. **673**, (2001)
12. S.P. Baker, M. P. Knauss, U.E. Mockl and E. Arzt, Mat. Res. Soc. Symp. Proc. Vol. **356**, 483-488 (1995)

13. R.I. Barabash, G.E. Ice, B.C. Larson, W. Yang, Rev. of Scientific Instrum., **73**, 1652 (2002).

FIGURE CAPTIONS:

Figure 1. Evolution of the (222) and (113) Laue reflections (in q-space) of four grains during the *in-situ* EM experiment. For each reflection, the area of q-space is kept constant, with length of a side given in  $\text{\AA}^{-1}$ .

Figure 2. (a) Peak broadening ( $\Delta\theta$ ) for individual grains along the length of the line 24 hours into the *in-situ* EM experiment ( $I = +30$  mA). (b) Grain rotations for individual grains on the top ( $y > 0$ ) and bottom ( $y < 0$ ) halves of the line versus position along the line. The convex bowing of the line increases as the anode is approached.

Figure 3. Average deviatoric stresses and average maximum resolved shear stress (MRSS) within the line versus time during the *in-situ* EM experiment. The different applied currents are delineated with the vertical dashed lines.

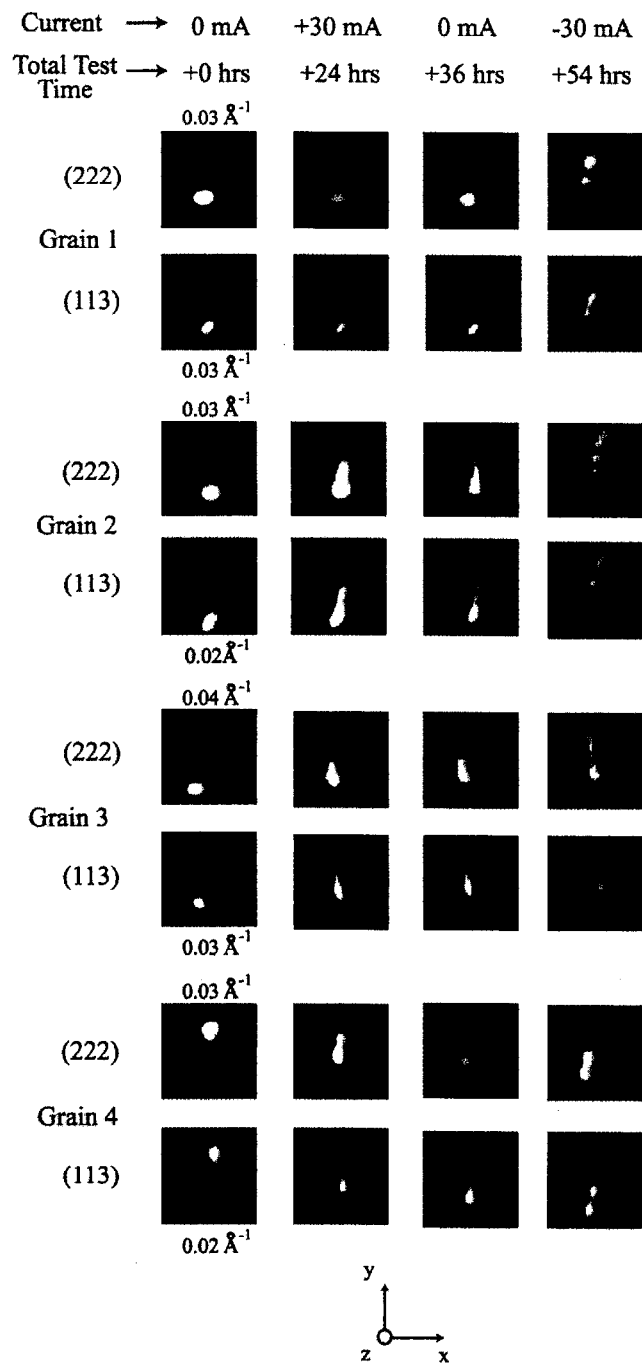


Figure 1.

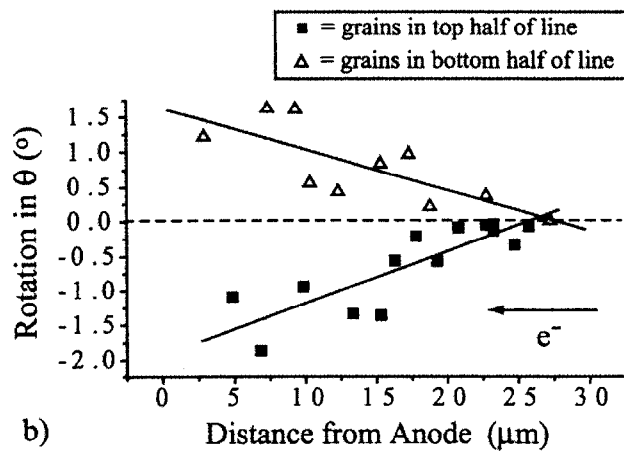
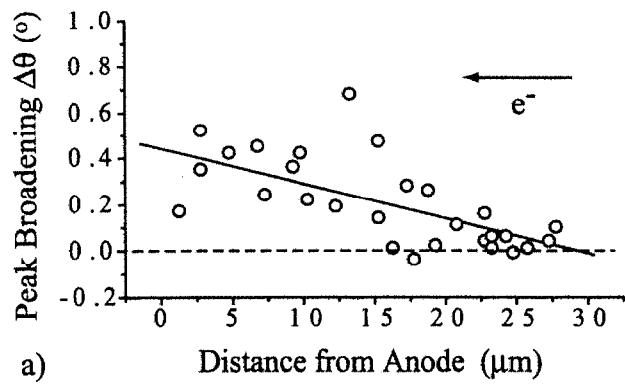


Figure 2.

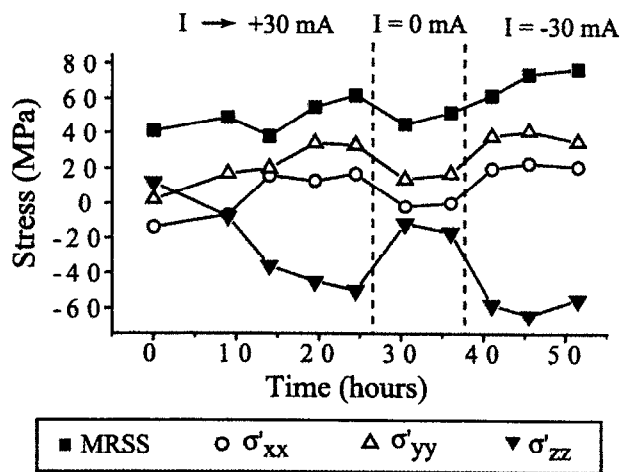


Figure 3